Anat Embryol (2005) 210: 387–400
DOI 10.1007/s00429-005-0030-8

ORIGINAL ARTICLE

O. Schmitt · J. Modersitzki · S. Heldmann
S. Wirtz · L. Hömke · W. Heide · D. Kömpf · A. Wree

Three-dimensional cytoarchitectonic analysis of the posterior bank of the human precentral sulcus

Published online: 22 September 2005

Abstract Studies employing functional magnetic resonance imaging have identified the human frontal eye field as being in the anterior and partly in the posterior wall, as well as at the base of the precentral sulcus. Moreover, it is known that the frontal eye field extends rostrally to the superior frontal sulcus. According to Brodmann's cytoarchitectonic map, this region belongs to the dysgranular Brodmann area 6 of the premotor cortex. However, the frontal eye field in non-human primates has been located within the arcuate sulcus in Brodmann area 8, generating considerable debate about where to locate exactly the frontal eye field in humans. Functional studies of the primate frontal eye field have revealed a principal homology of voluntary saccadic control systems in human and old-world monkeys, especially the macaque. But these homologies seem to be contradicted by the reported topographic localization at the cytoarchitectonic level. Therefore, we studied the cytoarchitectonic structure of the posterior bank of the precentral sulcus of a human brain, employing newly developed spatial mapping techniques to provide data about whether or not this region should be considered cytoarchitecturally homogeneous or heterogeneous. We used functional magnetic resonance imaging results, as an initial guide in localizing a region which is activated by saccadic tasks. A maximum of activation was detected around the junction of the superior frontal sulcus and the precentral sulcus extending 1.5 cm along the precentral sulcus in direction of the lateral sulcus. Here, one human brain has been analyzed to obtain preliminary data about the cytoarchitectonical changes of a part of area 6. Statistical analysis of the three-dimensional architectonic data from this region allowed us to identify a zone at the posterior bank, which in other studies has been associated with a functional region that controls pursuit eye movements and performs sensory-to-motor transformations. We found two significant sectors along the ventral part of the posterior bank of the precentral sulcus. The caudal transition region coincides partly with a region that integrates retinal and eye position signals for target location, arm, and axial movements. The second more ventrally located region is attributed to process oral-facial movements. The caudal transition region coincides with our functional magnetic resonance imaging investigation. It was revealed that this region lies at the inferior frontal eye field, where a pronounced activation over a larger region can be stimulated. Currently, more studies are needed to combine functional magnetic resonance imaging data of maximal activation with data from whole histologic brain sections of more individuals and to quantify the variability of this region and its sub-regions by means of a standardized brain atlas.

Keywords Human brain · Frontal eye field · Brodmann's area 6·Mapping · Precentral sulcus · Superior frontal sulcus · fMRI · Cytoarchitectonic mapping

O. Schmitt (✉) · A. Wree
Institute of Anatomy, University Rostock, Gertrudenstr. 9, D-18055 Rostock, Germany
E-mail: schmitt@med.uni-rostock.de
Tel.: +49-381-4948408/2

J. Modersitzki
Mathematics Science Center, Emory University, Suite W401, 400 Dowman Drive, Atlanta, GA, 30322 USA

S. Heldmann · S. Wirtz
Institute of Mathematics, University Lübeck, Wallstraße 40, D-23560 Lübeck, Germany

L. Hömke
Institute of Medicine, Research Center Jülich, D-52425 Jülich, Germany

W. Heide
Department of Neurology, AKH-Celle, Siemensplatz 4, D-29223 Celle, Germany

D. Kömpf
Department of Neurology, University Lübeck, Ratzeburger Allee 160, D-23538 Lübeck, Germany

Abbreviations 3D: three-dimensional · BA: Brodmann's area · BOLD: blood oxygen level dependent · CS: central sulcus · EPI: echo planar imaging · FEF: frontal eye field · FOV: field of view · iFEF: inferior frontal eye field · fMRI: functional magnetic resonance imaging · L: layer, lamina · LIP: lateral intraparietal area · MNI: Montreal Neurologic Institute · MRI: magnetic resonance imaging · NeuN: neuronal nuclear protein · PET: positron emission tomography · PCS: precentral sulcus · PMd: dorsal superior premotor cortex · PMd-caudal: caudal part of the dorsal premotor cortex · PMd-rostral: rostral part of the dorsal premotor cortex · PMv: ventral inferior premotor cortex · PMv-caudal: caudal part of the ventral premotor cortex · PMv-rostral: rostral part of the ventral premotor cortex · Pocg: postcentral gyrus · ROI: region of interest · Prcg: precentral gyrus · SEF: supplementary eye field · sFEF: superior frontal eye field · SWM: spatial working memory task · T1: longitudinal relaxation time · TE: echo time · TR: repetition time · VOI: volume of interest

Introduction

The discovery of the frontal eye field (FEF) and further eye fields of the cerebral cortex was first described by Ferrier (1875), who performed electrical stimulation of the frontal lobe of the macaque monkey brain and observed a movement of the eyes to the contralateral side. Further studies have located the FEF and supplementary eye field (SEF) in the brains of these primates (*Macaca fascicularis, Macaca mulatta*) and shown that the FEF lies along the dorsal part of the arcuate sulcus, as part of Brodmann's area (BA) 8 while the SEF is in the dorso-medial frontal lobe anterior to the supplementary motor area (Stanton et al. 1989, 1993, 1995). A third region, the parietal eye field, is located in the lateral intra-parietal area.

The FEF is primarily concerned with eye movements that serve to image important scenes of the visual world on the fovea of the retina (foveation) (Chalupa and Werner 2004), and it is the main cortical area for generation of all types of voluntary saccades, as well as for smooth pursuit eye movements (Chalupa and Werner 2004). Functionally, the FEF elicits saccades in general, including subtypes of visually guided saccades and self-paced saccades (Sweeney et al. 1996; Muri et al. 1998; Heide et al. 2001).

In *hominidae* (e.g., gorilla [*Gorilla gorilla*], orangutan [*Pongo pygmaeus*], chimpanzee [*Pan troglodyte*]) the frontal lobe does not possess an arcuate sulcus (Brauer and Schober 1970). Thus, the location and function of the human homologue of the FEF has been a matter of debate for many years (for a review see Schall 1997; Tehovnik 2000). However, electrical stimulation of a region behind, within, and before the precentral sulcus (PCS) of the human brain has been shown to provoke eye movements (Penfield and Jasper 1954; Godoy et al. 1990; Lobel et al. 2001; Blanke and Seeck 2003). Furthermore, there seems to be a cortical map directing movement that is implemented within the PCS (Rasmussen and Penfield 1948).

Studies using positron emission tomography (PET) to determine the regional cerebral blood flow have shown that in contrast with the FEF of macaque monkeys, the human FEF is not located in BA 8 but instead in a region where BA 6 should be expected (Fox et al. 1985; Petit et al. 1993, 1996; Anderson et al. 1994; Paus 1996). fMRI experiments at a higher spatial resolution have provided evidence that the FEF in humans is located around the lateral part of the PCS, extending above its junction with the superior frontal sulcus involving adjacent areas of the precentral gyrus (O'Driscoll et al. 2000; Heide et al. 2001; Rosano et al. 2002).

As reported by Ono (1990), the sulcus pattern of this region is complex and displays a high inter-individual variability. The author also identified four principal types of sulcus patterns that are not necessarily symmetrical with respect to the left and right hemispheres. Taking these characteristics into consideration, we find it difficult to provide a general prediction of the exact location of the FEF in an individual brain at the macroscopic level of gyrus and sulcus extensions.

Generally speaking, the FEF lies in the vicinity of the PCS and/or in the depth of the caudalmost part of the superior frontal. In a review of several PET-studies, Paus (1996) summarizes the coordinates of the FEF in Talairach–Tournoux-space (Tailarach and Tournoux 1993). It ranges for both hemispheres in the rostro-caudal direction from −6 to 1 mm (*y*-axis), dorso-ventral between 44 and 51 mm (*z*-axis), and in the medio-lateral direction for the left hemisphere from −24 to −40 mm and for the right one from 21 mm to 40 mm. Recent high-resolution fMRI studies (Courtney et al. 1998; Luna et al. 1998; Berman et al. 1999; Petit and Haxby 1999; O'Driscoll et al. 2000; Heide et al. 2001) suggest that the FEF seems not to extend anterior to the PCS into the middle frontal gyrus—the so-called oculogyric area—as previously reported (Duke-Elder and Wybar 1961), or/and BA 8 (Foerster 1931), or myeloarchitectonic region 55 (Vogt 1926). Instead, the FEF appears to be located more dorsal within the frontal lobe. Indeed, higher-resolution research and new experimental paradigms for fMRI studies (Heide et al. 2001) have demonstrated the existence of two separate portions of the FEF along the PCS: (i) a superior, dorso-medial portion centered at the superior part of the PCS and extending dorsally toward the posterior end of the superior frontal sulcus, and (ii) an inferior, ventro-lateral portion centered around the middle part of the PCS and extending into the precentral gyrus (Duvernoy 1999; Picard and Strick 2001; Rizzolatti et al. 2002). The location of oculomotor-related activity in these distinct regions of the PCS but not in areas rostral to it suggests a functional specialization of these cortical areas as being exclusive to the human FEF.

Previous cytoarchitectonic studies defined such regions, as homogeneous parts of the premotor cortex, which are dysgranular and agranular, respectively, as well as transitional and they do not differentiate the PCS from adjacent rostral regions (Brodmann 1909; Bailey and von Bonin 1951). However, other investigators have observed distinct rostral–occipital differences, which were designated as F***B*** , F***C*** *(**B**)* and F***C*** region (von Economo and Koskinas 1925); 6a, 6, 6p and 6op regions (Sarkissov et al. 1955); 39bL, 38b, 39bβ, 39c, 40β, 40L, 42d-L and 44a regions (Ngowyang 1934); 6aα, 6aβ, 6bα and 6bβ regions (Vogt and Vogt 1919; Foerster 1931); the frontomotoric zone of Sanides consists of five sub-regions: 37–42 (Sanides 1962) (Table 1). Descriptive myeloarchitectonic investigations differentiated up to eight areas (Vogt 1910: area 38–44, 55) (Strasburger 1937: 37–39, 41a, 42, 44, and 55b) and a quantitative mapping study (Schmitt et al. 2004a) provided evidence of a subdivision of BA 6 into rostro-occipital parts. At the very least, pigmentarchitectonic findings present a convincing argument for the existence of a homogeneous region (Braak 1980).

How and where to delineate subregions within BA 6, and where to locate the boundaries of the FEF at the cytoarchitectonic level, are challenging questions. Yet immuno-histochemical investigations using high-resolution fMRI and stereological quantification have provided some answers (Rosano et al. 2002, 2003). These investigations provided evidence for the location of the human FEF at the lip and anterior wall extending into the depth of the PCS and partly extending to its posterior bank (Picard and Strick 2001; Rizzolatti et al. 2002; Rosano et al. 2002).

However, Rosano et al. (2003) characterized the human FEF according to the comparative presence and distribution of neuronal nuclear protein, calbindin, calretinin and nonphosphorylated neurofilament by means of immuno-histochemistry. But current knowledge remains insufficient with respect to the spatial extension and its inter-individual variability. Recently developed mapping techniques operating on complete series of histologic sections at high spatial resolutions (Schmitt et al. 2002, 2003) are promising and they provide more detailed structural information about the spatial location of cytoarchitectonic FEF compartments.

As a cytoarchitectonic clue, the FEF can be characterized in humans (Rosano et al. 2002, 2003) and primates (Stanton et al. 1989, 1993, 1995; Rosano et al. 2002, 2003) by the appearance of clusters of large pyramidal cells in layer V and clusters of small pyramidal cells in layer III. But at present, no statistical analysis at the cytoarchitectonic level has been performed to determine the transition region of the FEF (Schmitt et al. 2003).

The search for the human FEF beyond PET and fMRI resolutions at the cytoarchitectonic level is necessary for understanding the structural and functional organization of the oculomotor system in humans. Furthermore, exact location of the human FEF and cytoarchitectonic characterization will be crucial to the success of connectivity studies and functional investigations at the molecular level.

The patterns of gyrus–sulcus-extensions at the junction of the superior frontal sulcus and the PCS, the distributed activation centers (Heide et al. 2001) and the problems of inter-individual variations of the superior and the inferior PCS interrupted by a gyrus crown demands a scrupulous step-by-step investigation of the different cortical parts in this and surrounding regions.

Table 1 The subdivision of BA 6 based on cytoarchitectonic and myeloarchitectonic studies in men and monkeys (modified from Schieber 1999)

Generic name	Generic abbreviation	Authors Brodmann (1909)	Vogt and Vogt (1919)	von Bonin and Bailey (1947)	Barbas and Pandya (1987, 1989)	Matelli et al. (1985, 1991)	Geyer et al. (2000)
		Species					
		Human, Cerocopithecus	Human, Macaca mulatta	Human, Macaca mulatta	Macaca nemestrina	Macaca fascicularis	Macaca nemestrina
Dorsocaudal part of the premotor cortex	PMd-caudal, PMdc	6	6aα	FB	6Dc	F2	F2
Supplementary motor area proper	SMA proper, SMAp	6	6aα	FB	6Dc	F3	F3
Ventrocaudal part of the premotor cortex	PMv-caudal, PMvc	6	6aα	FBA	6Va	F4	F4d, F4v
Dorsorostral part of the premotor cortex	PMd-rostral, PMdr	6	6aβ	FC	6Dr	F7	F7
Pre-supplementary area	pre-SMA, Psma	6	6aβ	FC	MII	F6	F6
Ventrorostral part of the premotor cortex	PMv-rostra, PMvrl	6	6b-α, 6b-β	FCBm	6Vb	F5	F5

Our objective is to develop a framework for spatial mapping at the cytoarchitectonic level of the posterior bank of the PCS, based on our fMRI studies, and to present the first results of an architectonic parcellation of this part of BA 6.

Materials and methods

Histology

The brain of a 70-year-old female (Body Donor Program, Institute of Anatomy, University of Lübeck, Germany) was dissected 4 h after death (Fig. 1). A whole brain immersion fixation in Somogyi fixans (Somogyi and Takagi 1982) was performed for 48 h to preserve the specimen for later immuno-histochemical studies (Schmitt et al. 2004b). A tissue block containing the posterior bank of the PCS was fixed in the same fixans for 7 days, after which the specimen was dehydrated and then embedded in paraffin wax. A total of 726 sections exhibiting a thickness of 20 µm were processed and then stained by the Gallyas method for perikarya (Fig. 2, 3, and 4). The direction of sectioning was parallel to the lateral convexity of the right hemisphere (Fig. 1, 2).

Image acquisition and analysis

All sections were digitized with a transparent flat bed scanner (Agfa®, Duoscan T2500) at an internal resolution of 12.7 µm/pixel. These scans (Fig. 3a) were preprocessed to obtain images containing only those parts of the cortex, which were of interest (Fig. 3b). The pial surface as the outer border and the white matter border were delineated in each section (Fig. 3c). This was followed by a calculation of test lines (traverses) (3d) running orthogonal through the cytoarchitectonic layers (Schmitt and Böhme 2002) to provide a profile array for each section (Fig. 3e). A profile is a distribution of gray values through which the ordinate is oriented orthogonal to the cytoarchitectonic layers and the abscissa indicates the intensity of pixels. The profile provides a characteristic pattern at each part of the cortex under investigation. The distance between

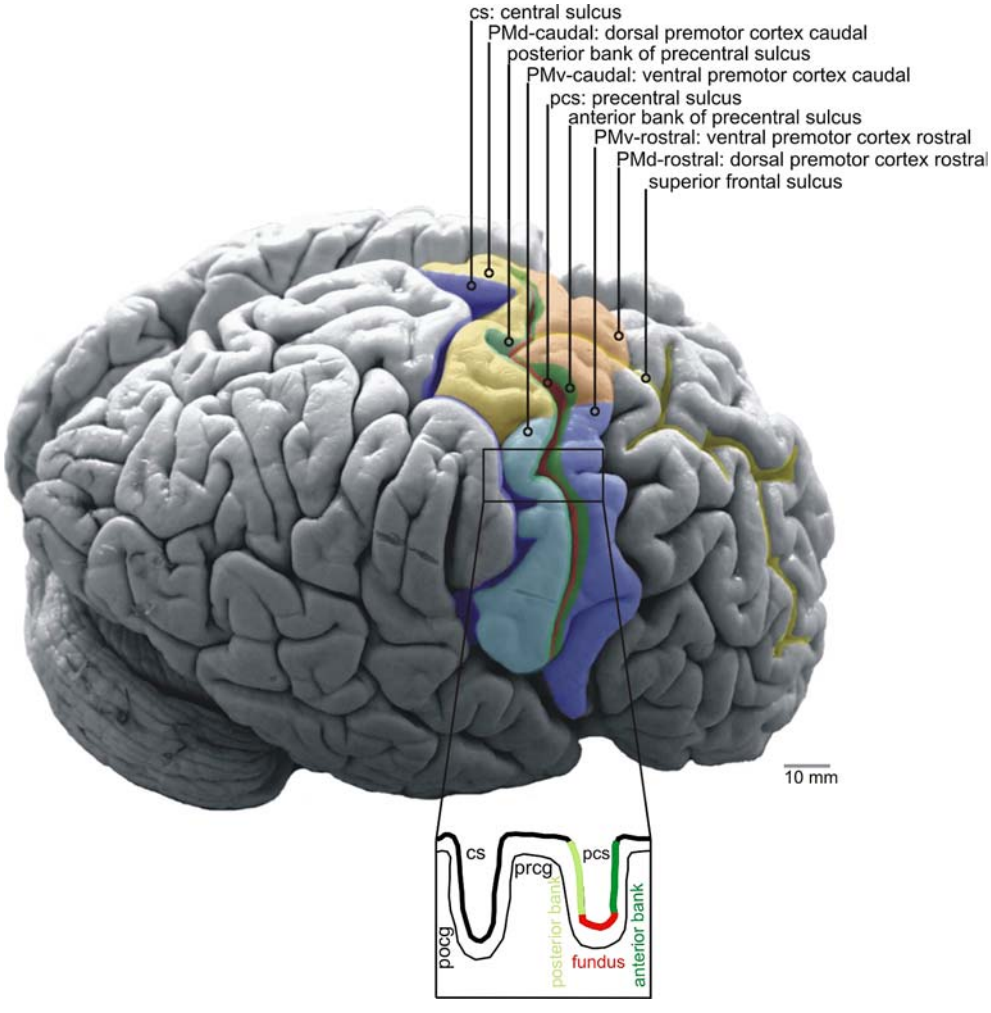

Fig. 1 The right hemisphere of the brain was investigated in this study. The subdivision of the premotor cortex into four sectors is shown. The superior frontal sulcus (*thin yellow line*), the precentral sulcus (*thin red line*), and the central sulcus (*blue line*) are displayed as well. An enlarged view of the precentral sulcus with the terms 'anterior bank' and 'posterior bank' is given below

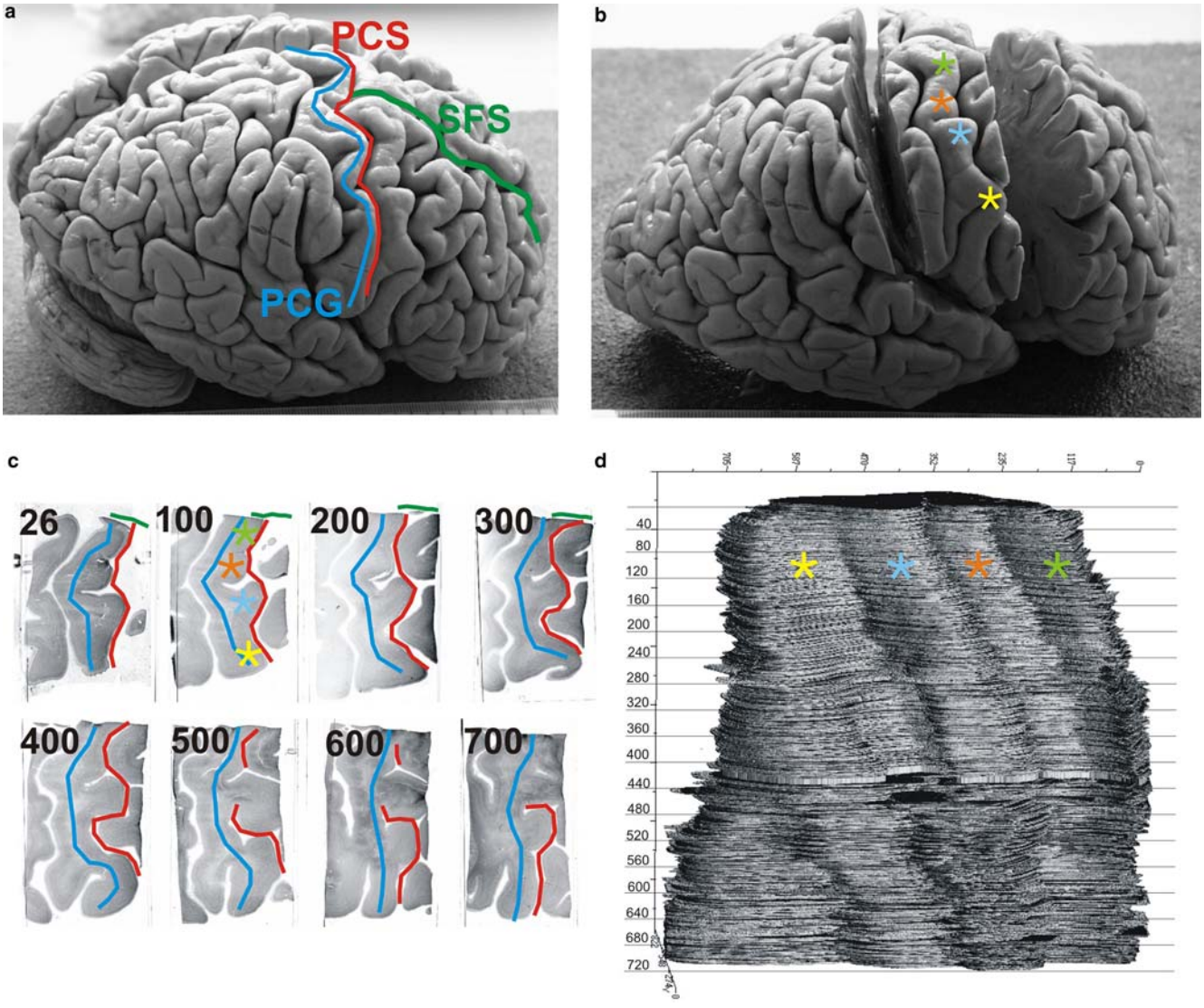

Fig. 2 a-d The steps of dissection and reconstruction are documented. The location of the precentral sulcus (*PCS*), superior frontal sulcus (*SFS*), and the precentral gyrus (*PCG*) are marked in **(a)**. On the tissue block, which has been sectioned serially, four star shaped markers lying on the PCG are shown in **(b)**. Eight sections 2 mm apart with the marker lines for the PCG, PCS, and SFS having the same colors as those in **(a)** are presented in **(c)**. Additionally, section number 100 has been marked with the stars having the same projective location like that in **(b)**. The same markers, as in **(b)** and of section 100 in **(c)** are used in the 3D-reconstruction of the image stack **(d)**. The reader is looking to the posterior wall of the reconstructed precentral gyrus

the traverses was the same as the internal resolution of the images.

These profile arrays were statistically analyzed after calculating differences of excess masses or areas under the local peaks of each profile using the multiple rank test (Fig. 3f) (Schmitt et al. 2003). The statistical analysis provided significant ($p \leq 0.05$) changes of the profile structure in small cortical regions, e.g., zones containing an increase or decrease of excess mass differences. The frequency of significant changes of excess mass differences are displayed in interval assays for increasing differences (upward jumps) and decreasing differences (downward jumps) (Fig. 3f).

For each profile array, a complex pattern of significant excess mass difference changes had to be interpreted, because the test is unable to differentiate among geometrical distortions introduced by extreme concavities and convexities, as well as artifacts such as tissue cracks, folds, and staining inhomogeneities or anomalies. These potential difficulties can affect study and analysis results and can at present only be detected by the observer.

With 726 profile arrays to review, we limited our analytical extractions to those arrays (1–510) derived from sections that show a continuous progression of cortex of the posterior wall. In Fig. 2c, section 500 shows an interrupt of the continuity of the posterior bank of the PCS, therefore, the following sections were not evaluated statistically. The interval assays (Fig. 3f) displaying either significant upward or downward jumps

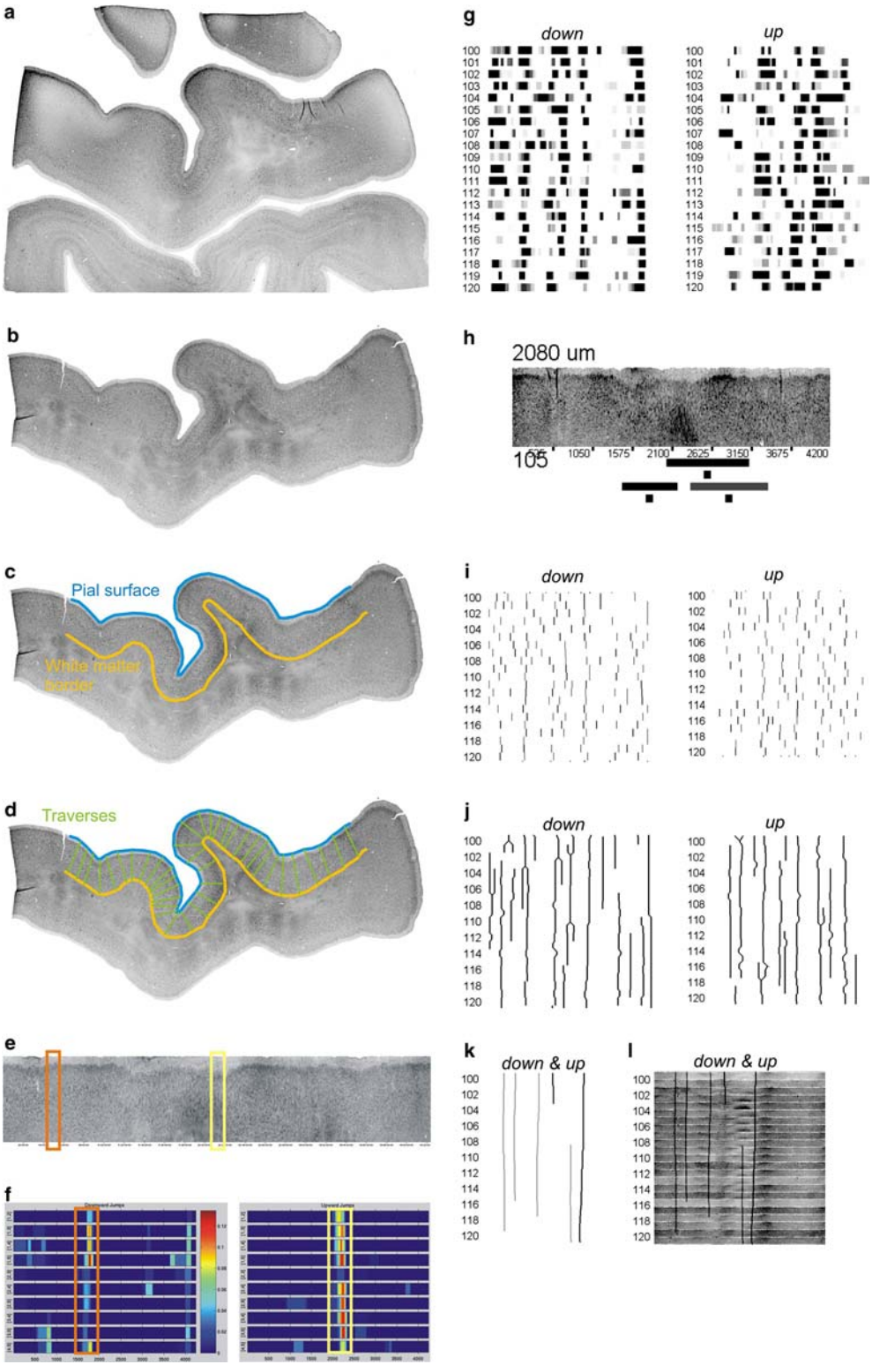

Fig. 3 a-f The steps of image preprocessing and data analysis: after digitizing and pre-segmentation **(a)** the region of interest **(b)** is transferred into a new image. Thereafter, the pial surface and the white matter border are assigned interactively **(c)** followed by calculation of orthogonal testlines, i.e., traverses **(d)**. The pixel intensities hit by the traverses are transferred into vectors, which present profiles or an array of profiles **(e)**. These profile arrays were statistically analyzed by searching for significant changes of excess mass differences indicated by rectangles in the interval diagrams of significances **(f)**. The information of the interval diagrams for decreases (*down jumps*) and increases of excess mass differences (*upward jumps*) are summed up over all interval combinations resulting in stripes of significances for the profile array of each section (section numbers are shown on the left of the stripes for downward and upward jumps **(g)**. Mean locations (*small rectangles*) of the stripes of significances (*large bars*) are computed **(h)**. In order to determine adjacent mean locations **(i, j)** of stripes of significances in neighboring sections, they were merged **(j)**. Branches were divided and the resulting lanes **(k)** were superimposed on the stack of profile arrays (*lanes of clustered significances*)

of excess mass differences were summed up over all intervals. The resulting stripes of significance (Fig. 3g) deliver an overview of the distribution and frequency of significances for the ROI of each section. To find out which significances overlap between adjacent profiles or sections, we calculated their mean. In Fig. 3h, a profile array with stripes derived from upward and downward jumps with their calculated mean positions are shown. Mean positions of stripes (Fig. 3i) derived from downward and upward jumps were evaluated with respect to their locations in adjacent sections. Thus, we obtained lanes of significances (Fig. 3j) over the sections under

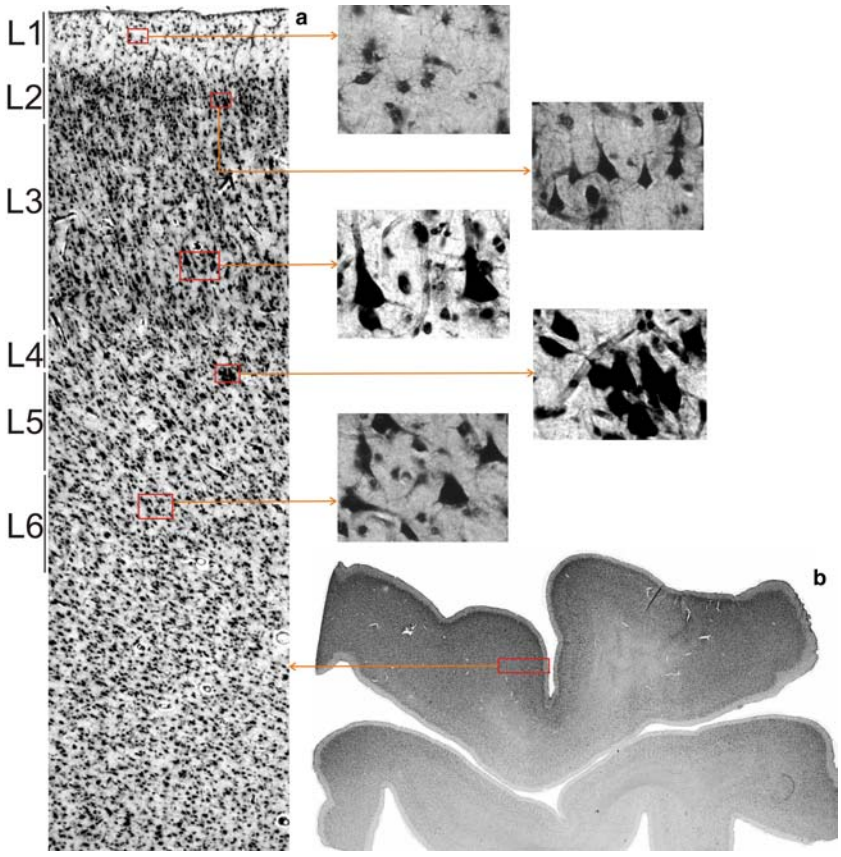

Fig. 4 a, b Micro- and mesoscopic views of section146, respective sections of the upper part of the posterior wall of the precentral sulcus are shown. In **(a)** the cytoarchitecture with layers indicated on the left are enlarged from the overview shown in **(b)**. The typical cytoarchitectonic features of the layers 1–6 are magnified on the upper right. The typical feature of clusters of large pyramidal cells, which was observed at the anterior wall of the PCS within the FEF was also found at the posterior wall in layer 5. Because layer 6 is sectioned tangentially a clear border to layer 5 is not visible

investigation. Lanes that lying apart were smoothed to visualize only those zones of significances that are concentrated in a restricted domain (Fig. 3k). A combination of these significant lanes and their appropriate profile arrays are shown in Fig. 3l. The significant lanes were evaluated over sections 1–510 in order to detect those zones where relative long lanes appear meaning that significant and stable structural changes occur at similar locations over several sections (Fig. 5).

Finally, the significant changes of cytoarchitectonic microstructure were visualized in a three-dimensional (3D)-reconstruction of the image stack (Fig. 6). For this reconstruction, the images were resampled to a size of 512×512 pixels, whereby images must be homogenized in order to reduce stronger staining inhomogeneities of adjacent sections. The homogenization was applied to the first- and second-order moments of the gray value statistic of the region that is covered by the section and which also may contain background intensities. An affine linear registration model was used after robust principal axes transformation (Modersitzki 2004). Rotation, translation, scaling, and shearing components were optimized to minimize the sum of squared differences between the images. The calculated borders of the cortical area exhibiting significant changes were mapped onto the surface and onto an orthogonal section of the 3D-reconstructions. Finally, the spatial distribution of significant upward and downward jumps of interval combinations are visualized in two 3D-reconstructions (Fig. 6d) displaying the detected transition regions from the statistical point of view.

Computations and visualizations were performed by using Matlab 6.5 (Mathworks Inc., Natiek, MA, USA) and T3D (Fortner Research, Sterling, VA, USA) on an Intel system operating with Linux or Windows XP.

Functional magnetic resonance imaging was done as described in the publication of Heide et al. (2001). In this study, triple-step stimuli and double-step stimuli were applied to six individuals to trigger memory-guided saccades. Furthermore, self-paced saccades in the darkness, visually guided saccades, single-memory-guided saccades, and a spatial working memory task were tested. The data obtained by the fMRI studies were used for locating macroscopically the most probable region in the postmortem brain that may contain the FEF.

Results

In the fMRI experiments, significant activations ($p \leq 0.01$) of the superior and mesial PCS were observed after performing triple-step saccades (Heide et al. 2001). Due to the inherent limitations of resolution, it is unclear if the activation maximum is located in the anterior or posterior bank of the PCS. More precisely, two activation maxima have been found. The superior activation, the superior frontal eye field (sFEF) is indicated by a red arrow and lies directly behind the orifice of the

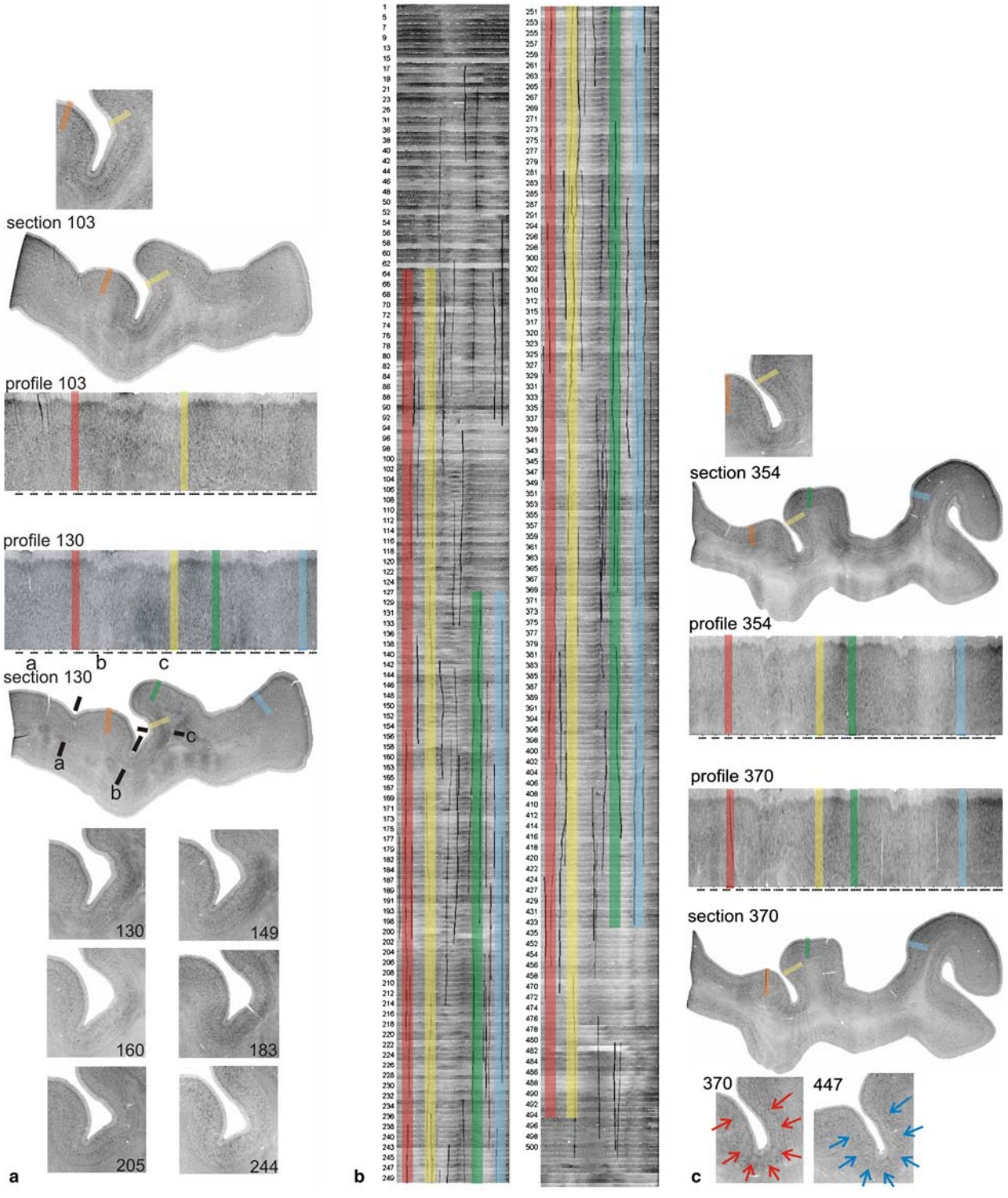

Fig. 5 a–c Those lanes of clustered significances which are overlapping are highlighted by *black lines* **(b)**. There exist two regions of overlapping significances that are longer than other. The first one is enclosed by a transparent *red and a yellow stripe* and the second one by a transparent *blue and a green stripe*. These stripes are shown in sections 103, 130, 354, 370 **(a, c)** and in magnified ROIs to compare significances with morphology. At the bottom of **(c)** *red arrows* are pointing to layer 3 containing scattered large pyramidals and *blue ones* to layer 5 exhibiting the clusters of large pyramidals

superior frontal sulcus. The inferior activation, the inferior frontal eye field (iFEF) is indicated by a yellow arrow and is located adjacent to the inferior frontal sulcus separated by the precentral gyrus. The MNI-coordinates of the maxima of activation of the left sFEF are −32, 48, and −4 (*x*: sagittal, *y*: coronal, *z*: axial) and

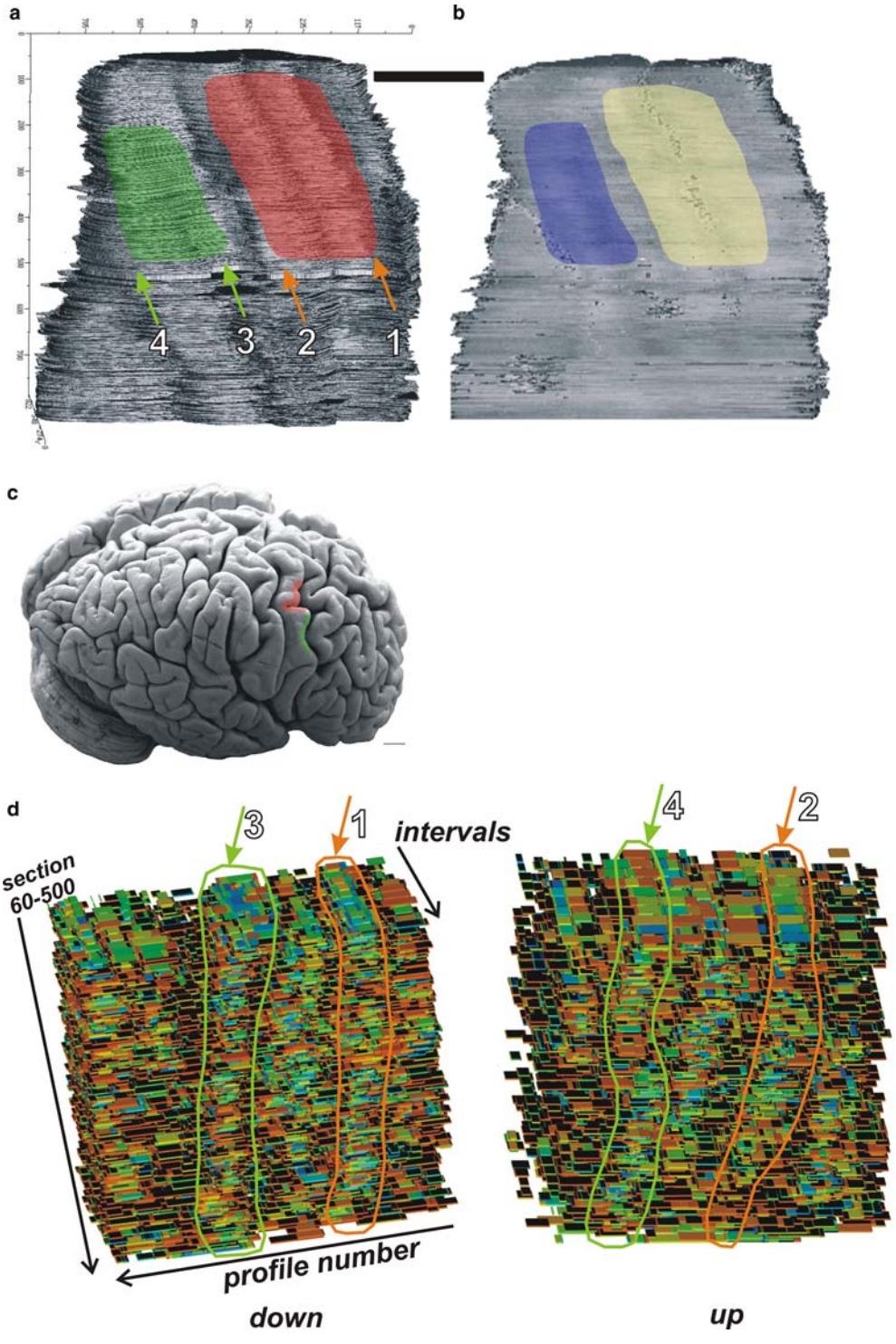

Fig. 6 a–c The three dimensional reconstruction of the stack of images facing the posterior wall of the precentral sulcus **(a)** and an orthogonal section through the reconstruction **(b)** is presented. The reconstruction has been marked by two regions as determined by significances indicating structural changes of cytoarchitecture in Fig. 5. The projection of the same region is marked at the crown of the precentral gyrus in the image of the brain before the tissue block was dissected **(c)**. An overview of a three-dimensional reconstruction of significant downward and upward jumps provides information of the extension of the two disjunct areas **(d)**. The significances corresponding to the dorsal region (*red*, low profile numbers) are indicated by numbered *orange arrows* (1, 2) and to the ventral region (*green*, large profile numbers) are pointing *green arrows* (3, 4). The first structural change of the dorsal region is indicated in the downward jump visualization **(d)** by an *orange arrow* pointing to a stack of significant changes with high spatial frequency. The ventral transition of region 1 can be found in the upward jump visualization indicated by an *orange arrow*. The ventral transition of region 2 is found in the downward jump visualization (*green arrow*) and the dorsal transition in the upward jump visualization

of the right sFEF are 32, 52, and 0. The maxima of activation of the left iFEF are −48, 36, and 0 and those of the right iFEF are 44, 44, and −4.

Furthermore, activations could be observed not only at the junction of the PCS and superior frontal sulcus but also about 10 mm downward along the PCS. These two small activations appeared approximately 1 cm and 2 cm, respectively, caudal from the region where the strongest activation had been measured.

The inspection of the cytoarchitecture at the posterior bank adjacent to the location of activation, as described above, reveals cytoarchitectonic features that comprise similarities like those of macaque monkeys

FEF. In a region that is located caudal to the superior frontal sulcus within the middle and lower part of the posterior bank of the PCS, large pyramidal cells in layer V forming small groups of three to six cells are conspicuous. Furthermore, clusters of large pyramidal cells in layer III were found (Fig. 4a).

The matching of significances ($p \leq 0.05$) over all sections revealed two pairs of accumulation of indicative measurements, one at profile positions 1000 (downward jumps) and 2000 (upward jumps) and a second at 2500 (downward jumps) and 4200 (upward jumps) (Fig. 5). A prime significance of the data concerning these two transition regions is that the first regions had the same locations beginning at section 64 and the second region starting at section 127. That means that this structural change had a distance of ± 2 mm (region 1) and ± 3.2 mm (region 2) under the crown of the precentral gyrus. Moreover, from here, region 1 appeared over a distance of 8 mm and region 2 over a distance of 6 mm into the depth of the PCS. Additionally, in the tissue block under investigation, the transition region 1 was typically located around a small notch which could be tracked down the PCS (Fig. 4). Within region 1 delineated by the accumulations of significances, we observed clusters of large pyramidal cells in layer 5, which are magnified in Fig. 4a and indicated in the enlarged parts of the investigated images in Fig. 5c. This feature was lacking in region 2.

Further accumulations of significances were found at the basin of this small notch (Fig. 5). They are located in Fig. 6b, as black stripes surrounded by the red and yellow stripes, which indicate the transition regions. These significances were most probably caused by the geometry of the concave-like dip. However, others were more caudal but not to the extent that one would have expected for a cytoarchitectonic transition region.

The extension of these two cytoarchitectonic disjunct regions were projected on the 3D-reconstruction of the stack of segmented and registered images (Fig. 6). Region 1 is highlighted in red and region 2 in green. Their lateral extensions are mapped on the surface of the precentral gyrus in Fig. 6c. Both regions are lying in PMvc or F4. Statistical significant changes of excess mass differences are visualized in three dimensions to facilitate recognition of regularities in comparison to stacks of significances as shown in Fig. 5b. The transition regions are visible within the volume of interest (VOI) as stacks of red, green and blue stained rectangles containing the whole statistical information, i.e., frequency of significances, interval (combination of excess mass differences), and spatial extension (Fig. 6d). The statistical VOI of downward jumps shows transition 1 of region 1 and the VOI of upward jumps transition 2 of region 1. Furthermore, transition 1 of region 2 was visualized in the VOI of downward jumps and transition 2 of region 2 in the VOI of upward jumps.

Discussion

The exact spatial location, extend and shape of the human FEF can not be determined by either structural or functional MRI-investigations. However, fMRI-measurements of activations induced by saccadic tasks were conducted in this study to determine the approximate location of activations, which were observed along the PCS either on the posterior or anterior wall. Two maxima of activations induced by a saccadic task were related to the sFEF and the iFEF. Additionally, small activations were found more ventrally in the PCS. Due to the limited resolution of the fMRI technique, it is not clear whether the maxima of activation are located at the anterior and/or the posterior wall.

In a first approach, we investigated these regions within the posterior wall of the PCS. The cytoarchitecture of the posterior bank of the inferior PCS was analyzed in consecutive sections parallel to the lateral hemispheric convexity by a statistical analysis of changes of excess mass differences in profile arrays. Because we obtained information of significant changes of the cytoarchitectonic structure within each section, this information can be compared section-by-section in order to determine those significances that appear regularly around the same relative location. However, anomalies resulting from small folds (Figs. 3, 5) of the cortical surface were preserved and those must be distinguished from structural changes emanating from the cytoarchitectonic pattern.

The anterior and posterior bank of the PCS are divided into a dorsal or superior premotor cortex (PMd) and a ventral or inferior premotor cortex (PMv) (Picard and Strick 2001) (Fig. 1, Table 1). With respect to the anterior-posterior direction, these regions are subdivided into a part belonging to the anterior (PMd-rostral, PMv-rostral) and the posterior bank (PMd-caudal, PMv-caudal) of the PCS (Rizzolatti et al. 2002) (Fig. 1, Table 1) resulting in a four-quadrants like arrangement. Furthermore, the PMd-caudal contains a ventrorostral or rostrolateral sector and the PMv-rostral was subdivided into three subregions (Matelli and Luppino 1996). It should be emphasized, that the mentioned structural and functional parcellations are based on studies in maquace monkeys.

In contrast to the primary motor cortex, which solely processes motor aspects of task performance, the PMd plays a preferential role in sensory or context-dependent processing of a task performance (Shen and Alexander 1997).

More specifically, the PMd is involved in the selection and planning of visually guided movements (Crammond and Kalaska 1996), which seems to be realized in a restricted subarea lying ventrorostral or rostrolateral in the PMd-c (Fogassi et al. 1999). PMd performs sensory-to-motor transformations, which combine retinal and eye position signals for target localization (Andersen et al. 1985, 1990; Zipser and Andersen 1988; Bremer

et al. 1997a, 1997b, 1998) and the combination of movement with preparatory signals with eye position for movement representation (Boussaoud and Bremmer 1999).

The PMv can be subdivided into three distinct regions (Gabernet et al. 1999) in the macaque monkey brain, and it is somatotopically organized whereby axioproximal movements are generated by the caudal part and distal movements are located more rostrally. Since the macaque region F4 and the inferior PCS are homologous of the PMv and the descending branch of the inferior PCS of humans (Fadiga et al. 2000), it is likely that these structures can be compared directly from a functional perspective.

In general, two populations of neurons can be differentiated within the PMv, both of which are related to movement execution but one of them has direct access to the spinal motor apparatus (Hepp-Reymond et al. 1994). Furthermore, it was observed that there exists a congruent relationship between the location of visual fields and preferred arm movements (Genticulli et al. 1988).

In summary, the PMd seems to realize the interface between eye movements and motor control, while the PMv appears as a supplemental system of the primary motor cortex, albeit with a modified somatotopy and integrative subfunctions.

In this study, two regions contiguous to the activations observed in the fMRI-experiments on the posterior bank of the PCS were detected that exhibit significant structural changes in comparison with adjacent parts of BA 6 containing the dorsally and superiorly located PMd and the ventrally and inferiorly located PMv. The regions identified by statistical analysis of excess mass differences are located more rostrally in the PMv (posterior bank of the PCS). We found two structurally distinct sectors in PMv-caudal or F4. It is known that this region has a course somatotopic motoric organization, i.e., arm and axial movements are controlled in the upper or dorsal part and oral-facial movements in the lower part (Gentilucci et al. 1988, 1989; Rizzolatti et al. 1988, 1990). It is most probable that the transitions of the structural features of cytoarchitectonics of the two regions found by us coincide with these two parts of the PMv-caudal.

Recently, the superior part of the anterior bank (PMd-rostral) was investigated by immunohistochemistry of nonphosphorylated neurofilament, calcium binding proteins, and neuronal nuclear protein (Rosano et al. 2003) (Fig. 1). This group found a cytoarchitectonic pattern, which is comparable with those described by Stanton et al. (1989), i.e., large pyramidal cells in deep layer III, small groups of three to six large pyramidal cells in layer V at the lower half of the anterior wall, including the fundus of the precentral gyrus. These small groups of large pyramidal cells were never observed within the crown or the most caudal part of the precentral gyrus and this feature in addition with the loosely distributed large pyramidal cells in deep layer III is considered as a typical pattern of the FEF. Nevertheless, clusters of large layer V cells appear in both walls of the PCS (Rosano et al. 2003). This phenomenon was also observed by us, as shown in Fig. 4.

A 3.0 T high-resolution fMRI investigation of saccadic and slow pursuit eye movements with emphasis of BOLD-signal location and with respect to the anterior and posterior bank was conducted (Rosano et al. 2002). It has been shown convincingly that the maximum of activity during saccadic eye movement is located within the upper part and lip of the anterior wall of the superior PCS. Pursuit eye movements produce a maximum of activation within the fundus of the PCS.

Furthermore, pursuit eye movements have been observed to produce a slight asymmetry of activation with a pronouncement of the right hemisphere. Activity during saccadic and pursuit eye movements also was observed within the posterior wall. However, the difference of signal intensity of the anterior and posterior wall was determined to be significant. Nevertheless, these zones of activation at the posterior bank may be co-activated within saccadic eye movements and for pursuit eye movements. The transition regions found by us match exactly into these zones of activation.

The maximum of activation of the fMRI investigation during saccading eye movements is located at the upper half of the anterior wall with extension into the superior frontal sulcus (Rosano et al. 2002), whereby this region contains the feature of clustering of large pyramidal cells in layer V typic for the FEF. Rosano et al. (2003) found this feature also in deeper portions of the posterior PCS wall. The later observation can be confirmed in this study. The conspicuous feature of pyramidal cell clustering within layer V seems to be located with highest density of the upper half of the anterior PCS wall and then with decreasing density to the fundus of the PCS up to the posterior PCS wall. With respect to the aggravating circumstance of interindividual variability of this region, where the frontal superior sulcus meets the superior PCS this assumption of the distribution of pyramidal clusters has to be proved. It is indispensable to perform a cytoarchitectonic mapping study based on activation maxima of visomotoric tasks and data of different individuals, which are transformed into a normalized brain atlas coordinate system (Amunts et al. 2004). Nevertheless, this appears to be a challenge because the walls of the PCS performing a twisted way. Coronal sections through such a gyrus landscape will offer multiple, more or less tangential sections of the walls which will render more difficult an analysis by means of cortical scanning as presented here. However, developing a 3D scanning of registered histological sections will facilitate the analysis of frequently tangentially sectioned transition regions.

The stack of sections investigated by us was not registered before generating the profile arrays, because they have an external resolution of 7,000×3,000 pixels. The resulting dataset is far too large for correcting

elastic deformations using an intra-modal method without an external reference such as a morphologic MRI-scan of the tissue. In order to maintain spatial relations among the profile arrays, they were aligned indirectly by selecting the start and the stop location for the traverse generation, which have the same position in adjacent sections.

Also, because we defined the start and stop of the outer contour line at the pial border and the inner contour line at the white matter border, the profile arrays have a sufficient alignment primarily for quantitative comparisons. However, it is necessary and intended for the future to perform an affine and elastic registration before profile arrays will be generated. Such a registration will have to be performed carefully and diligently since a reference-free elastic registration may introduce unexpected distortions which may affect the statistical evaluation of the excess mass differences.

The new approach of analyzing stacks of contiguous histologic sections at high spatial resolutions is an effective method for investigating complex cytoarchitectonics around the PCS. According to our observations typical cytoarchitectonic features of the human FEF can be observed partly at the posterior bank of the PCS. To determine the extension of this part of the cerebral cortex exhibiting these features in confining gyral walls, it is necessary to investigate cytoarchitectonics in three dimensions over a series of contiguous histologic sections. The inter-individual variability and spatial extent of the FEF can be studied applying the 3D-approach presented here in individual brains with consecutive normalization of the results to an atlas brain.

Conclusions

The human premotor cortex lying around the PCS covered mostly by Brodmann area 6 is not composed of a homogeneous cytoarchitecture. Different investigators have delineated different sectors that partly coincides with different functions like control of saccadic eye movements. However, to our knowledge, there exists no study investigating the cytoarchitecture of the precentral walls by means of observer-independent statistical analysis of the cytoarchitectonics in three dimensions.

Therefore, we performed a 3D analysis of the cytoarchitecture of the posterior bank of the PCS applying statistical evaluation of excess mass differences of a region of interest of each section. The stack of digitized histologic sections have been preprocessed by image analysis, registered, and mapped onto a 3D-reconstruction of them. Overlapping significances that form clusters within consecutive sections were matched to obtain information of their spatial extension. Two significant regions were located at the inferior posterior wall of the PCS covering an area of 2 mm in parallel with the lateral convexity and 8 mm into the depth of the PCS. These regions are most likely associated with a motoric representation of the upper extremity and oral-facial movements. Within this study, we established a new method for analyzing cytoarchitecture in three dimensions at high resolution.

An important challenge is expected by the determination and location of structure–function-correlations and there inter-individual variability by mapping significant cytoarchitectonic inhomogeneities in three dimensions derived from different individuals onto a standardized atlas of the human brain.

Acknowledgement We thank U. Almert and P. Lau of the Institute of Anatomy (University of Lübeck) for excellent histologic preparations. Dr. F. Binkofski and Dr. M. Nagel were of great help, as they provided the activation maxima of saccadic experiments. We also thank S. Haas for support and M. Westlund for editing of the manuscript.

References

Amunts K, Weiss PH, Mohlberg H, Pieperhoff P, Eickhoff S, Gurd JM, Marshall JC, Shah NJ, Fink GR, Zilles K (2004) Analysis of neural mechanisms underlying verbal fluency in cytoarchitectonically defined stereotaxic space–the roles of Brodmann areas 44 and 45. Neuroimage 22:42–56

Andersen RA, Essick GK, Siegel RM (1985) Encoding of spatial location by posterior parietal neurons. Science 230:456–458

Andersen RA, Bracewell RM, Barash S, Gnadt JW, Fogassi L (1990) Eye position effects on visual, memory and saccade related activity in areas LIP and 7A of macaque. J Neurosci 10:1176–1196

Anderson TJ, Jenkins IH, Brooks DJ, Hawken MB, Frackowiak RS, Kennard C (1994) Cortical control of saccades and fixation in man. A PET study. Brain 117:1073–1084

Bailey P, von Bonin G (1951) The isocortex of man. University of Illinois Press, Urbana, IL

Barbas H, Pandya DN (1987) Architecture and frontal cortical connections of the premotor cortex (area 6) in the rhesus monkey. J Comp Neurol 286:211–228

Barbas H, Pandya DN (1989) Architecture and intrinsic connections of the prefrontal cortex in the rhesus monkey. J Comp Neurol 286:353–375

Berman RA, Colby CL, Genovese CR, Voyvodic JT, Luna B, Thulborn KR, Sweeney JA (1999) Cortical networks subserving pursuit and saccadic eye movements in humans: an fMRI study. Hum Brain Mapp 8:209–225

Blanke O, Seeck M (2003) Direction of saccadic and smooth eye movements induced by electrical stimulation of the human frontal eye field: effect of orbital position. Exp Brain Res 150:174–183

von Bonin G, Bailey P (1947) The neocortex of *Macaca mulatta*. University of Illinois Press, Urbana, IL

Boussaoud D, Bremmer F (1999) Gaze effects in the cerebral cortex: reference frames for space coding and action. Exp Brain Res 128:170–180

Braak H (1980) Architectonics of the human telencephalic cortex. Springer, Berlin Heidelberg New York

Brauer K, Schober W (1970) Catalogue of Mammalian Brains. VEB Gustav Fischer Verlag, Jena

Bremmer F, Ilg UJ, Thiele A, Distler C, Hoffmann K-P (1997a) Eye position effects in monkey cortex. I. Visual and pursuit related activity in extrastriate areas MT and MST. J Neurophysiol 77:944–961

Bremmer F, Distler C, Hoffmann K-P (1997b) Eye position effects in monkey cortex. I. Pursuit- and fixation-related activity in posterior parietal areas LIP and 7A. J Neurophysiol 77:962–977

Bremmer F, Pouget A, Hoffmann K-P (1998) Eye position encoding in the macaque posterior parietal cortex. Eur J Neurosci 10:153–160
Brodmann K (1909) Vergleichende Lokalisationslehre der Grosshirnrinde in ihren Prinzipien dargestellt auf Grund des Zellenbaues. Barth, Leipzig
Chalupa LM, Werner JS (eds) (2004) The visual neuroscience. MIT Press, Cambridge
Courtney SM, Petit L, Maisog JM, Ungerleider LG, Haxby JV (1998) An area specialized for spatial working memory in human frontal cortex. Science 279:1347–1351
Crammond DJ, Kalaska JF (1996) Differential relation of discharge in primary motor cortex and premotor cortex to movements versus actively maintained postures during a reaching task. Exp Brain Res 108:45–61
Duke-Elder S, Wybar KC (1961) The anatomy of the visual system. Henry Kimpton, London
Duvernoy HM (1999) The human brain surface, blood supply, and three-dimensional sectional anatomy. Springer, Wien
von Economo C, Koskinas GN (1925) Die Zytoarchitektonik der Hirnrinde des erwachsenen Menschen. Springer, Wien
Fadiga L, Fogassi L, Gallese V, Rizzolatti G (2000) Visuomotor neurons: ambiguity of the discharge or 'motor' perception? Int J Psychophysiol 35:165–177
Ferrier D (1875) Experiments on the brains of monkeys. Proc R Soc Lond 23:409–432
Foerster O (1931) The cerebral cortex in man. Lancet 2:309–312
Fogassi L, Raos V, Franchi G, Gallese V, Luppino G, Matelli M (1999) Visual responses in the dorsal premotor area F2 of the macaque monkey. Exp Brain Res 128:194–199
Fox PT, Fox JM, Raichle ME, Burde RM (1985) The role of cerebral cortex in the generation of voluntary saccades: a positron emission tomographic study. J Neurophysiol 54:348–369
Gabernet L, Meskenaite V, Hepp-Reymond MC (1999) Parcellation of the lateral premotor cortex of the macaque monkey based on staining with the neurofilament antibody SMI-32. Exp Brain Res 128:188–193
Gentilucci M, Fogassi L, Luppino G, Matelli M, Camarda R, Rizzolatti G (1988) Functional organization of inferior area 6 in the macaque monkey. I. Somatotopy and the control of proximal movements. Exp Brain Res 71:475–490
Gentilucci M, Fogassi L, Luppino G, Matelli M, Camarda R, Rizzolatti G (1989) Somatotopic representation in inferior area 6 of the macaque monkey. Brain Behav Evol 33:118–121
Geyer S, Matelli M, Luppino G, Zilles K (2000) Functional neuroanatomy of the primate isocortical motor system. Anat Embryol 202:443–474
Godoy J, Luders H, Dinner DS, Morris HH, Wyllie E (1990) Versive eye movements elicited by cortical stimulation of the human brain. Neurology 40:296–299
Heide W, Binkofski F, Seitz JR, Posse S, Nitschke MF, Freund H-J, Kömpf D (2001) Activation of frontoparietal cortices during memorized triple-step sequences of saccadic eye movements: an fMRI study. Eur J Neurosci 13:1177–1189
Hepp-Reymond MC, Husler EJ, Maier MA, Ql HX (1994) Force-related neuronal activity in two regions of the primate ventral premotor cortex. Can J Physiol Pharmacol 72:571–579
Lobel E, Kahane P, Leonards U, Grosbras M, Lehericy S, Le Bihan D, Berthoz A (2001) Localization of human frontal eye fields: anatomical and functional findings of functional magnetic resonance imaging and intracerebral electrical stimulation. J Neurosurg 95:804–815
Luna B, Thulborn KR, Strojwas MH, McCurtain BJ, Berman RA, Genovese CR, Sweeney JA (1998) Dorsal cortical regions subserving visually guided saccades in humans: an fMRI study. Cereb Cortex 8:40–47
Matelli M, Luppino G (1996) Thalamic input to mesial and superior area 6 in the macaque monkey. J Comp Neurol 372:59–87
Matelli M, Luppino G, Rizzolatti G (1985) Patterns of cytochrome oxidase activity in the frontal agranular cortex of the macaque monkey. Behav Brain Res 18:125–136
Matelli M, Luppino G, Rizzolatti G (1991) Architecture of superior and mesial area 6 and the adjacent cingulate cortex in the macaque monkey. J Comp Neurol 311:445–462
Modersitzki J (2004) Numerical methods for image registration. Oxford University Press, Oxford
Muri RM, Heid O, Nirkko AC, Ozdoba C, Felblinger J, Schroth G, Hess CW (1998) Functional organization of saccades and antisaccades in the frontal lobe in humans: a study with echo planar functional magnetic resonance imaging. J Neurol Neurosurg Psychiatry 65:374–377
Ngowyang G (1934) Die Cytoarchitektonik des menschlichen Stirnhirns. Monogr Nat Res Inst Psychol Acad Sin 7:1–69
O'Driscoll GA, Wolff AL, Benkelfat C, Florencio PS, Lal S, Evans AC (2000) Functional neuroanatomy of smooth pursuit and predictive saccades. Neuroreport 11:1335–1340
Ono M, Kubik S, Abernathey CD (1990) Atlas of the cerebral sulci. Thieme, Stuttgart
Paus T (1996) Location and function of the human frontal eye-field: a selective review. Neuropsychologia 34:475–483
Penfield W, Jasper H (1954) Epilepsy and the functional anatomy of the human brain. Little Brown and Co, Boston
Petit L, Haxby JV (1999) Functional anatomy of pursuit eye movements in humans as revealed by fMRI. J Neurophysiol 82:463–471
Petit L, Orssaud C, Tzourio N, Salamon G, Mazoyer B, Berthoz A (1993) PET study of voluntary saccadic eye movements in humans: basal ganglia-thalamocortical system and cingulate cortex involvement. J Neurophysiol 69:1009–10017
Petit L, Orssaud C, Tzourio N, Crivello F, Berthoz A, Mazoyer B (1996) Functional anatomy of a prelearned sequence of horizontal saccades in humans. J Neurosci 16:3714–3726
Picard N, Strick PL (2001) Imaging the premotor areas. Curr Opin Neurobiol 11:663–672
Rasmussen T, Penfield W (1948) Movement of head and eyes from stimulation of human frontal cortex. Res Publ Assoc Res Nerv Ment Dis 27:346–361
Rizzolatti G, Camarda R, Fogassi L, Gentilucci M, Luppino G, Matelli M (1988) Functional organization of inferior area 6 in the macaque monkey. II. Area F5 and the control of distal movements. Exp Brain Res 71:491–507
Rizzolatti G, Gentilucci M, Camarda RM, Gallese V, Luppino G, Matelli M, Fogassi L (1990) Neurons related to reaching-grasping arm movements in the rostral part of area 6 (area 6a beta). Exp Brain Res 82:337–350
Rizzolatti G, Fogassi L, Gallese V (2002) Motor and cognitive functions of the ventral premotor cortex. Curr Opin Neurobiol 12:149–154
Rosano C, Krisky CM, Welling JS, Eddy WF, Luna B, Thulborn KR, Sweeney JA (2002) Pursuit and saccadic eye movement subregions in human frontal eye field: a high-resolution fMRI investigation. Cereb Cortex 12:107–115
Rosano C, Sweeney JA, Melchitzky DS, Lewis DA (2003) The human precentral sulcus: chemoarchitecture of a region corresponding to the frontal eye fields. Brain Res 972:16–30
Sanides F (1962) Die Architektonik des menschlichen Stirnhirns Monographien aus dem Gesamtgebiete der Neurologie und Psychiatrie: 98. Springer, Berlin Heidelberg New York
Sarkissov SA, Filimonoff IN, Kononowa EP, Preobraschenskaja IS, Kukuew LA (1955) Atlas of the cytoarchitectonics of the human cerebral cortex. Medgiz, Moscow
Schall JD (1997) Visuomotor areas of the frontal lobe. In: Rockland K, Peters A, Kaas J (eds) Extrastriate cortex of primates, vol 12, Cerebral cortex. Plenum Press, New York, pp 527–638
Schieber MH (1999) Somatotopic gradients in the distributed organization of the human primary motor cortex hand area: evidence from small infarcts. Exp Brain Res 128:139–148
Schmitt O, Böhme M (2002) A robust transcortical profile scanner for generating 2D-traverses in histological sections of rich curved cortical courses. Neuroimage 16:1103–1119
Schmitt O, Hömke L, Dümbgen L (2003) Detection of cortical transition regions utilizing statistical analysis of excess masses. Neuroimage 19:42–63

Schmitt O, Pakura M, Aach T, Hömke L, Böhme M, Bock S, Preuße S (2004a) Analysis of nerve fibers and their distribution in histologic sections of the human brain. Microsc Res Tech 63:220–243

Schmitt O, Preuße S, Haas SJP (2004b) Comparison of contrast, sensitivity and efficiency of signal amplified and nonamplified immunohistochemical reactions suitable for videomicroscopy based quantification and neuroimaging. Brain Res Methods 12:157–171

Shen L, Alexander GE (1997) Preferential representation of instructed target location versus limb trajectory in dorsal premotor area. J Neurophysiol 77:1195–1212

Somogyi P, Takagi H (1982) A note on the use of picric acid and paraformaldehyde glutaraldehyde fixative for correlated light and electron mircoscopic immuno-cytochemistry. Neuroscience 7:1779–1783

Stanton GB, Deng SY, Goldberg ME, McMullen NT (1989) Cytoarchitectural characteristics of the frontal eye fields in macaque monkeys. J Comp Neurol 282:415–427

Stanton GB, Bruce CJ, Goldberg ME (1993) Topography of projections to the frontal lobe from the macaque frontal eye fields. J Comp Neurol 330:286–301

Stanton GB, Bruce CJ, Goldberg ME (1995) Topography of projections to posterior cortical areas from the macaque frontal eye fields. J Comp Neurol 353:291–305

Strasburger E (1937) Die myeloarchitektonische Gliederung des Stirnhirns beim Menschen und Schimpansen. J Psychol Neurol 47:461–491

Sweeney JA, Mintun MA, Kwee S, Wiseman MB, Brown DL, Rosenberg DR, Carl JR (1996) Positron emission tomography study of voluntary saccadic eye movements and spatial working memory. J Neurophysiol 75:454–468

Talairach J, Tournoux P (1993) Referentially orientated cerebral MRI anatomy. Thieme Medical publishers Inc, New York

Tehovnik EJ, Sommer MA, Chou IH, Slocum WM, Schiller PH (2000) Eye fields in the frontal lobes of primates. Brain Res Brain Res Rev 32:413–448

Vogt O (1910) Die myeloarchitektonische Felderung des menschlichen Stirnhirns. J Psychol Neurol 15:221–238

Vogt O (1926) Die vergleichend-architektonische und die vergleichend-reizphysiologische Felderung der Großhirnrinde unter besonderer Berücksichtigung der menschlichen. Naturwissenschaften 14:1190–1194

Vogt C, Vogt O (1919) Allgemeine Ergebnisse unserer Hirnforschung. J Psychol Neurol 25:279–461

Zipser D, Andersen RA (1988) A back-propagation programmed network that simulates response properties of a subset of posterior parietal neurons. Nature 331:679–684